On the Structure and Dynamics of the Oceanic Bottom Boundary Layer

GEORGES L. WEATHERLY

Department of Oceanography and Geophysical Fluid Dynamics Institute, Florida State University, Tallahassee 32306

PAUL J. MARTIN

NORDA, Bay St. Louis, MS 35929

(Manuscript received 24 June 1977, in final form 13 March 1978)

ABSTRACT

The Mellor and Yamada (1974) Level II turbulence closure scheme is used to study the oceanic bottom boundary layer (BBL). The model is tested against observations of the BBL obtained on the western Florida Shelf reported in Weatherly and Van Leer (1977) and in turn conclusions about the BBL made in that paper are tested against the model. The agreement between the model and the observations is good. The predicted and observed BBL thickness is ~10 m which is appreciably less than $0.4\, u_*/f \approx 30$ m, where u_* is the friction velocity and f the Coriolis parameter. The reason for the discrepancy is attributed to the BBL being formed in water which initially was stably stratified and characterized by a Brunt Vasäilä frequency N_0. It is suggested that the oceanic BBL thickness should be identified with the height at which the turbulence generated in the BBL goes to zero and on dimensional grounds it is proposed that this thickness is $A\, u_*/f(1 + N_0^2/f^2)^{1/4}$, where A is a constant. The Level II model indicates that this is a good approximation over the range $0 \leq N_0/f \lesssim 200$ provided $A \approx 1.3$. Other features common to the predicted results and observations are 1) the vertical profiles of temperature and current direction which are very similar, with most of the direction changes (Ekman veering) occurring at the top of the BBL where the density stratification is largest; 2) a jet-like structure in some of the speed and direction profiles; and 3) appreciably more total Ekman veering than expected for a comparable BBL formed in neutrally stratified water.

The one-dimensional BBL formed under an along-isobath current in a stably stratified ocean is investigated for the case when the bottom is inclined relative to the horizontal isotherms. It is found that the BBL may no longer have the signature of a simple, vertically well-mixed layer because of Ekman-veering-induced upwelling (downwelling) of cooler (warmer) water in the BBL.

The profile of down-the-pressure gradient velocity component in the BBL is found to closely resemble the downslope flow of a heavier fluid discussed in Turner (1973). The Froude number stability criteria given in Turner (1973) when applied to the Level II model results suggest that the BBL formed in a stably stratified ocean is, in a Froude number sense, stable or marginally stable on continental margins while it is unstable in the deep ocean.

1. Introduction

Turbulent closure models are used to study the atmospheric boundary layer. A review of some of these models can be found in Mellor and Yamada (1974), and examples of their use can be found in Frenkiel and Munn (1974). An example of their efficacy is their general ability to reproduce the structure of neutrally stratified planetary boundary layers. The models have also been used to test theoretical predictions which at the time remained to be observationally confirmed. A case in point is the study of Businger and Arya (1974) which confirmed the prediction of Zilitinkivich (1972) that the height of the atmospheric boundary layer is proportional to $\mu_*^{-1/2}$ for the asymptotic case of large positive stability, where $\mu_* = u_*/|f|L$. Here u_* is the friction velocity, f the Coriolis parameter, and L the Monin-Obukhov length scale.

Turbulent closure models have been used, also with encouraging results, to study the oceanic surface mixed layer (Mellor and Durbin, 1975). We are aware, though, of only one study (Weatherly, 1975) where one of the more recent closure models using the turbulent kinetic energy equation has been used to study the benthic boundary layer (BBL). This work can be considered as a sequel to that preliminary study. In contrast to Weatherly (1975), the Mellor and Yamada (1974) turbulence closure scheme rather than the one developed by Vager and Zilitinkivich (1968) and extended by Lykosov and Gutman (1972) is used, and the results are compared to a different, more detailed data set. A study by one of us (Martin, 1976) indicates that the predictions of the Level II model and the Russian one used in Weatherly (1975) for the simple cases considered here are qualitatively similar and differ quantitatively due to different choices of critical Richard-

0022-3670/78/0557-0570$07.00

son number at which shear-generated turbulence is extinguished. For the Level II model this critical Richardson number is 0.23 while for the Russian model it is 1.0.

Section 2 is a review of the observations against which the numerical model is tested. In Section 3 the equations to be solved are presented, and in Section 4 the turbulence closure scheme used is reviewed and the method of solution discussed. The results in turn lead to two digressions, one on the general question of the thickness of the BBL formed in a stably stratified ocean and the other on the question of whether the BBL is stable in a Froude number sense. Section 6 is a summary and discussion.

While the numerical predictions are compared to observations, the objective of this study was to gain insight into the BBL formed in a stably stratified ocean, rather than to minimize the variance between predictions and observations. While we test the model against observation, we also use the model to test some of the conclusions drawn from observations which are presented in the next section. For these reasons we attempt to keep things simple when possible. For example, rather than use the observed velocity as the forcing term in the model, we approximate it as being constant.

2. Review of observations

In this section, some of the results given in Weatherly and Van Leer (1977, hereafter referred to as I, are reviewed. The data examined in I were obtained from a cyclesonde (Van Leer *et al.*, 1974) which was programmed to sample at ~2.5 m intervals in the vertical along a taut mooring line in water of depth ~101 m at 26° 0'N, 83° 49'W on the western Florida Continental Shelf. A total of 119 profiles of horizontal velocity, temperature and conductivity, made from ~3 m above the bottom to ~13 m from the surface between 3 and 8 July 1976, were examined. Since the BBL was the subject of I, only data obtained within ~50 m of the bottom were presented.

Sample profiles are shown in Fig. 1. There are four sets of temperature, σ_t, speed and direction profiles in Fig. 1; the first two are from the first part of the experiment when the flow away from the boundary was northward and approximately along the isobaths; the third set is from the middle part of the experiment when the interior flow was cross isobath and westward; and the fourth is from the last part of the experiment when the interior flow was again approximately along isobaths but southward. These

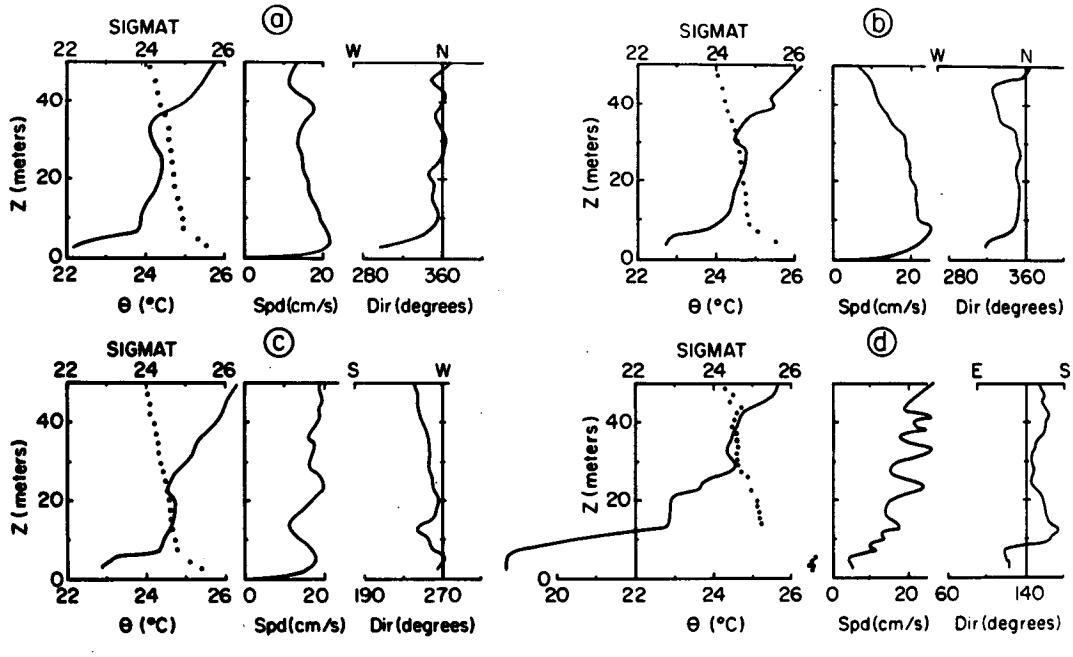

JOURNAL/MO/AU:

FIG. 1. Representative temperature, speed and current direction profiles taken from data reported in Weatherly and Van Leer (1977). Profiles (a) and (b) correspond to northward (along-isobath) interior flow when the temperature in the BBL increased with time. Profiles (c) were taken when the interior flow was westward and the temperature in the BBL was nearly constant with time. Profiles (d) correspond to southward (along-isobath) interior flow, during which period the temperature in the BBL decreased rather quickly with time. Dotted curves are σ_t profiles. Note that for $z \gtrsim 10$ m, $\partial\sigma_t/\partial z$ is nearly constant. The BBL is associated with the lens of relatively dense water for $z \lesssim 10$ m.

temperature, speed and direction profiles are typical of those obtained in that they show much vertical structure, which makes identification of the bottom boundary layer contentious. While the temperature profiles show much structure and suggest that near $z = 30$ m the water is unstably stratified, the σ_t or density profiles show that for $z \gtrsim 10$ m up to $z \approx 85$ m, the density gradient is nearly constant with a corresponding Brunt-Vasäilä frequency $N_0 = 7 \times 10^{-4}$ s^{-1}, while for $z \lesssim 10$ m there is a lens of relatively cold, salty, dense water.

The thickness of the bottom boundary layer h is often taken to be about

$$h = 0.4u_*/f \qquad (1)$$

(Wimbush and Munk, 1970; Weatherly, 1972; Kundu, 1976; Caldwell, 1976; Mercado and Van Leer, 1976). Estimating the friction velocity u_* by $0.03G$, where G is the magnitude of the geostrophic current outside the BBL (Weatherly, 1976), and taking $G = 0.15$ m s^{-1} (see Fig. 1) gives $h \approx 30$ m. However, in I it was concluded that h varied from about 6 to 12 m, considerably less than the estimate of 30 m. In I the thinner boundary layer was attributed to it being formed in stably stratified water.

From Fig. 1, certain patterns about the vertical structure of the BBL, assuming it was correctly identified in I, are indicated. Most of the direction changes occur in the upper part of the BBL where the temperature (density) stratification is largest. The total direction change across the BBL is larger than the 10–20° expected for a comparable turbulent Ekman layer formed in a neutrally stratified fluid [see Kundu (1976) and Mercado and Van Leer, (1976) for such estimates of Ekman veering]. The direction and temperature profiles were qualitatively similar. In some of the speed profiles there is an indication of a jet-like structure in the upper part of the BBL. A jet-like structure is also indicated in some of the direction plots as noted in I.

In I it was noted in the beginning of the experiment that when the interior flow was northward and oriented approximately along the isobaths, the temperature in the BBL increased at a faster rate than outside the BBL. When the interior flow was oriented across the isobaths during the period of westward flow, no consistent differential trend in warming or cooling of the BBL relative to the interior was apparent. However, in the latter part of the experiment, when the interior flow was again oriented approximately in the direction of isobaths but was southward, the temperature in the BBL decreased at a faster rate than that outside the BBL and the magnitude of temperature change in the BBL was greater for the period of southward interior flow. The warming in the BBL for the period of northward flow is indicated in Figs. 1a and 1b and the protrusion of a cold, dense lens above the bottom during southward interior flow is indicated in Fig. 1d. From the cyclesonde data, time series of temperature at fixed depths above the bottom were constructed. This information is shown in Fig. 2, taken from I, and illustrates the relative heating and cooling in the BBL ($z \lesssim 10$ m) in the periods of, respectively, northward (time $\lesssim 48$ h) and southward (time $\gtrsim 72$ h) flow.

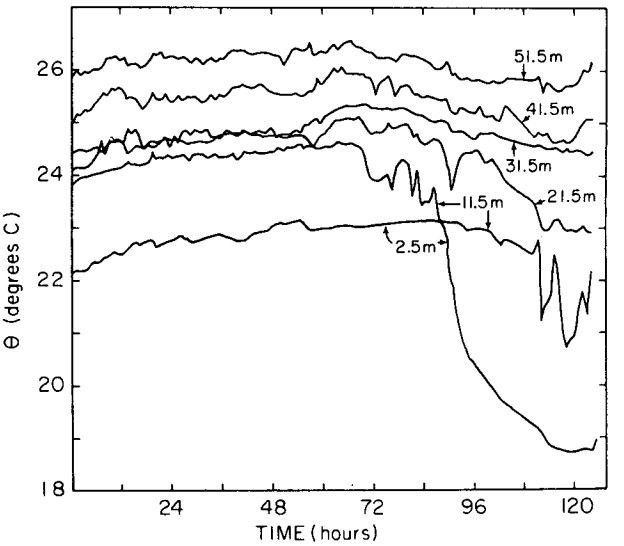

FIG. 2. Temperature-time series at various heights above the bottom, taken from Weatherly and Van Leer (1977). The interior flow was approximately northward for time $\lesssim 48$ h, westward for 48 h $\lesssim$ time $\lesssim$ 72 h and southward for time $\gtrsim$ 72 h.

In I it was suggested that the relative observed warming and cooling in the BBL could be due to, respectively, downwelling or upwelling in the BBL. Fig. 3, taken from I, shows a temperature, salinity and σ_t transect across the western Florida Shelf at 26°N, taken in June 1972. The site of the experiment (26° 0′N, 83° 49′W) is approximately at the shelf break point at 100 m depth. East of the site the bottom slope is about 0.26×10^{-3} and west of the site of the slope it is about 2.4×10^{-3}. At the site the isotherms (isopycnals) are approximately horizontal and intersect the bottom. In I it was proposed that if comparable conditions applied during the time of the cyclesonde observations, the BBL for an interior northward flow (into the plane of Fig. 3) could advect warmer downslope and hence could result in local heating of the BBL. Conversely, a southward interior flow could result in local cooling in the BBL. Since the appropriate bottom slope for upwelling is about an order of magnitude greater than that for downwelling (2.4×10^{-3} compared to 0.26×10^{-3}), it was argued in I that the magnitude of the observed BBL cooling should indeed be much larger than the observed BBL heating.

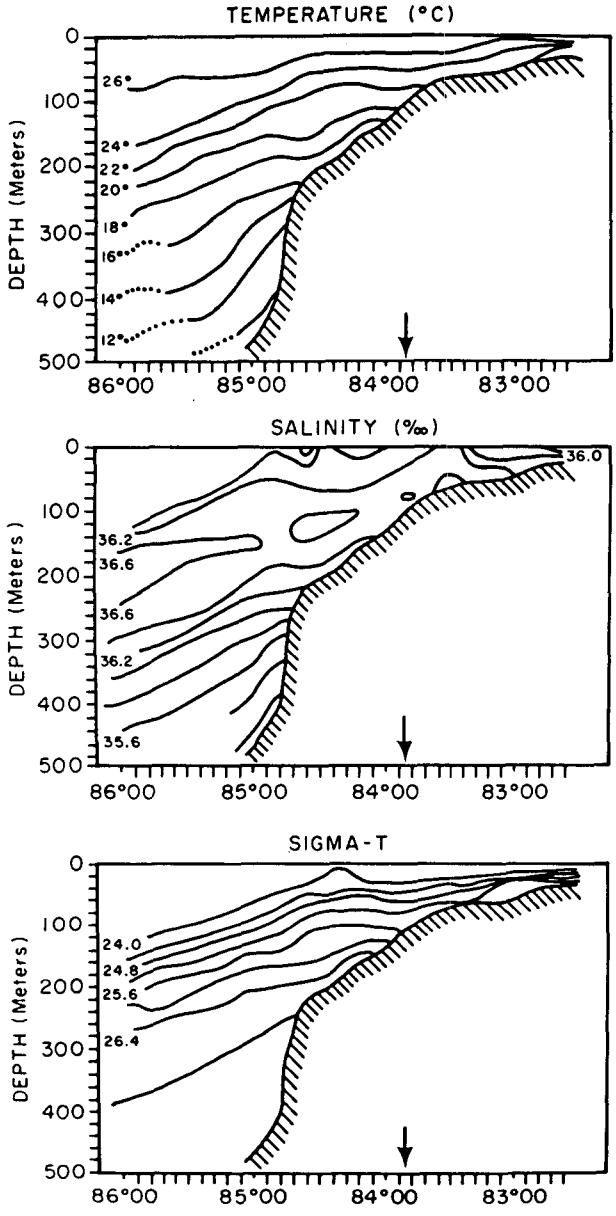

FIG. 3. Temperature, salinity and σ_t transect along 26°N on 2 June 1972 (courtesy of C. N. K. Mooers, University of Delaware, Lewes). The site of the observations (26°0'N, 83°49'W) is at 100 m depth and near a shelf break point where the bottom slope changes from 0.26×10^{-3} to 2.4×10^{-3}.

3. The equations

The problem we consider is sketched in Fig. 4. We assume that away from the boundary in the interior the flow is geostrophic and parallel to the bottom, that the isotherms are horizontal (no thermal wind), and that the temperature stratification is stable and constant. We further assume that in the bottom boundary layer all perturbations from the interior velocity, temperature and pressure fields are independent of horizontal position along the bottom and vary only with distance above the boundary. The bottom is allowed to be inclined at a constant angle relative to the interior isotherms and the coordinate axis is oriented so isobaths are parallel to the y axis.

With the above constraints the boundary layer equations are (Lykosov and Gutman, 1972)

$$\frac{\partial U}{\partial t} - fV = \frac{\partial}{\partial z}(-\overline{u'w'} + \nu \partial U/\partial z) + \alpha\lambda\Theta, \quad (2a)$$

$$\frac{\partial V}{\partial t} + fU = \frac{\partial}{\partial z}(-\overline{v'w'} + \nu \partial V/\partial z), \quad (2b)$$

$$\frac{\partial \Theta}{\partial t} + \alpha SU = \frac{\partial}{\partial z}(-\overline{\theta'w'} + \chi \partial \Theta/\partial z), \quad (3)$$

where z is the vertical coordinate relative to the flat bottom, t is time, U,V are velocity components relative to the geostrophic velocity components U_g,V_g, f is the Coriolis parameter, $-\overline{u'w'}$, $-\overline{v'w'}$ are Reynolds stresses, ν and χ are molecular diffusion coefficients for momentum and heat, α is the bottom slope (assumed small so $\sin\alpha \approx \alpha$, $\cos\alpha \approx 1$), λ is the buoyancy parameter (the thermal coefficient of expansion times gravity), Θ is the temperature relative to the initial temperature Θ_I, $S = \partial\Theta_I/\partial z$, and $-\overline{\theta'w'}$ is the turbulent heat flux divided by density ρ and heat capacity.

The boundary conditions which the solutions of (2) and (3) must satisfy are taken to be

$$U = -U_g, \quad (4a)$$

$$V = -Vg, \quad \text{at} \quad z = z_0, \quad (4b)$$

$$-\overline{v'w'} + Z(\partial\Theta/\partial z + S) = 0, \quad (4c)$$

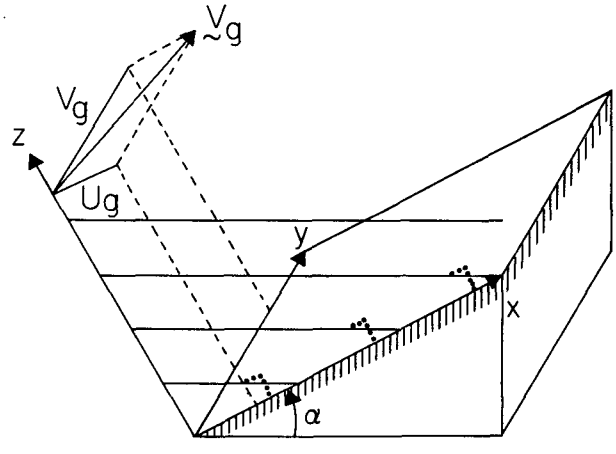

FIG. 4. Geometry considered. Isotherms are shown in the $y = 0$ plane where solid lines are Θ_I and the dotted lines the actual temperature Θ. In Eqs. (2) and (3) $\Theta = \theta - \Theta_I$. The geostrophic velocity is taken to be parallel to the flat bottom, Θ_I = constant lines are taken to be horizontal and $\partial\Theta_I/\partial z \equiv S$ is taken to be constant. The bottom is allowed to be tilted relative to east at the angle α.

where z_0 is the roughness parameter and

$$U \to 0, \tag{5a}$$

$$V \to 0, \tag{5b}$$

$$\Theta \to 0 \quad \text{as} \quad z \to \infty, \tag{5c}$$

$$\overline{u'w'} \to 0, \tag{5d}$$

$$\overline{v'w'} \to 0, \tag{5e}$$

$$\overline{\theta'w'} \to 0. \tag{5f}$$

The boundary condition (4c) is that of a thermally insulated bottom.

With the bottom slope zero ($\alpha = 0$) and the interior stratification nonzero ($S > 0$), the problem as posed in (2)–(5) has no steady solution. The temperature of the BBL continually increases with time due to the steady downward heat flux from the interior. The boundary condition (4c) precludes this heat from going out through the bottom. The assumption that U, V and Θ depend only on z and not x and y forces the local vertical velocity to be identically zero everywhere. Thus this heat cannot be advected back into the interior. A steady solution is of course possible if (4c) is changed so that the heat flux into the bottom matches that coming into the BBL from the interior. However, in this study we are concerned with time scales on the order of a week or less, rather than the case when $t \to \infty$. With $S = 7 \times 10^{-2}$ °C m^{-1}, $\chi \approx 10^{-7}$ m^2 s^{-1} and a BBL thickness of 10 m (see Section 5) the downward diffusion of heat from the interior leads to a warming of the BBL of about 6×10^{-5} °C day^{-1}. This heating in our "steady solutions" is ignored.

With the bottom slope non-zero ($\alpha \neq 0$) and the interior stratification non-zero ($S > 0$), Eqs. (1) and (2) are the equations for a buoyant Ekman layer. Hsueh (1969) and Lykosov and Gutman (1972) have considered steady, buoyant Ekman layers in the atmosphere for the case of constant eddy diffusivities. In these studies the temperature rather than the temperature gradient [see (4c)] was specified at the ground. However, their solutions are easily modified to satisfy a lower boundary condition on the temperature gradient, and the corresponding steady solutions to (2) and (3) subject to the boundary conditions (3)–(5) are

$$U = e^{-z/\delta}[-U_g \cos z/\delta - V_g(1 + \alpha^2 N_0^2/f^2)^{1/2} \sin z/\delta], \tag{6a}$$

$$V = e^{-z/\delta}[-V_g \cos z/\delta + U_g(1 + \alpha^2 N_0^2/f^2)^{1/2} \sin z/\delta] \tag{6b}$$

$$= (f/\alpha S)\Theta,$$

where $\delta \equiv /2K/f(1 + \alpha^2 N_0^2/f^2)^{-1/4}$ and $N_0^2 = \lambda S$ is the Brunt-Vasäilä frequency in the interior. Furthermore, the boundary condition (4c) requires that U_g and V_g be such that

$$U_g = (1 + \alpha^2 N_0^2/f^2)^{1/2}(-V_g + \delta f/\alpha). \tag{7}$$

In arriving at these solutions the constant eddy diffusivities of heat and momentum have been set equal to each other and equal to K. The expression (6) may be obtained from solving the system (2)–(5), setting $\overline{u'w'} = \overline{v'w'} = \overline{\theta'w'} = 0$ and $\nu = \chi = K$. Hereafter constant or variable K will denote constant or variable eddy diffusivities.

From these solutions we see that the natural time scale for a buoyant Ekman layer is not the inertial period $2\pi/f$ but rather $2\pi/F$, where $F = f(1 + \alpha^2 N_0^2/f^2)^{1/2}$. Thus the response time for a buoyant Ekman layer to attain equilibrium might be expected to be about $2\pi/F$ which $\leq 2\pi/f$. In this study we consider the BBL formed under steady currents which are oriented along isobaths, i.e., in cases where V_g = constant and $U_g = 0$ (see Fig. 4). However, from (7) it is apparent that no steady solution is possible in the constant K case when V_g = constant $\neq 0$ and $U_g = 0$. Thus, in the variable K case it might also be expected that in general no steady solutions to (2) and (3), subject to the boundary condition (4) and (5), are possible when V_g = constant $\neq 0$ and $U_g = 0$. Indeed, results presented later which simulate such conditions are clearly nonstationary even after times $\gtrsim 8\pi/F$ (~4 days) after the long isobath interior flow has reached its steady value. In contrast, our variable K model for comparable conditions with the bottom slope set equal to zero essentially attains steady-state conditions within one $2\pi/f$ period after the interior flow becomes constant.

This unsteadiness in a buoyant Ekman layer formed under a steady current flowing along isobaths is clearly seen in the temperature field. It is important to note that this unsteadiness in the temperature of the BBL is not due to the downward heat flux from the interior mentioned earlier but results instead from the Ekman-veering-induced advection of water upslope or downslope. For example with $\alpha > 0$ and a northward interior flow (i.e., $V_g > 0$, see Fig. 4) warmer water will be advected downslope resulting in a localized heating of the BBL. Conversely, with $\alpha > 0$ but the interior flow southward ($V_g < 0$), cooler water will be advected upslope leading to localized cooling of the BBL (cf. Figs. 5c and 5d). For the cases considered in this paper the net heating or cooling rate of the BBL due to this effect is many orders of magnitude greater than that due to the diffusion of heat into the BBL from the interior.

With K variable the BBL is expected to be well mixed in temperature and not surprisingly the turbulence closure scheme used here does give a bot-

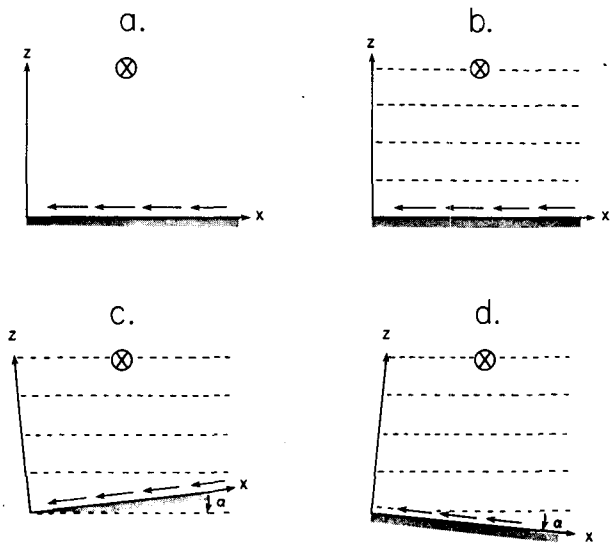

FIG. 5. The four BBL cases considered in Section 5. In all the cases, the interior flow has the same constant value and is directed into the plane of the figure. The direction of the cross-isobaric, Ekman-veered flow in the BBL is indicated by arrows. In the first case (a) there is no density stratification in the interior, $N_0^2 = 0$; in the second case (b) constant density stratification is included, $N_0^2 > 0$; and in the final two cases [(c) and (d)] the bottom is inclined relative to the horizontal isotherms. The case with positive bottom slope (c) corresponds to the northward interior flow discussed in Section 2 and that with negative bottom slope (d) corresponds to southward interior flow, also mentioned in Section 2.

tom mixed layer. For the case illustrated in Fig. 5c, using hindsight provided by the results of our model, this turbulent mixing is expected to keep temperature inversions from forming and hence the BBL from being warmer than the overlying water. However, as long as the temperature of the BBL increases with time due to cross-isobath Ekman veering the thickness of the BBL is expected to increase as well. By integrating (3) vertically through the BBL and applying the boundary conditions (4c) and (5f) it is seen that the temperature of the BBL will change with time if $\int^h U dz \neq \chi/\alpha$. For the case illustrated in Fig. 5d the temperature of the BBL will also continue to change with time as long as the cross-isobath Ekman transport does not equal χ/α. However, unlike the case shown in Fig. 5c the thickness of the BBL is not expected to change with time. Thus, while the buoyant bottom Ekman layer formed under a steady current for the simple examples shown in Figs. 5c and 5d is expected to be a well mixed layer, the temperature of the BBL is expected to change with time and the thickness of this BBL may also change with time.

4. The closure scheme and method of solution

a. The closure scheme

The purpose here is to briefly describe the closure scheme used to parameterize the vertical turbulent fluxes of momentum and heat in (2) and (3). We refer the reader to the papers cited in the section for more detail.

Mellor and Yamada (1974) presented a series of four turbulence closure schemes for planetary boundary layers labeled Level I to Level IV in order of increasing complexity. The models were developed through systematic scaling of the equations for the turbulent fluxes of heat and momentum. The modeling of the triple correlation and dissipation terms in these equations was based on hypotheses proposed by Rotta (1951) and Kolmogoroff (1941), and the values of constants used in such terms were determined from laboratory measurements of homogeneous turbulence. In a simulation of the diurnal variation of the atmospheric boundary layer, Mellor and Yamada found that the four models gave very similar results.

In modeling the BBL, we used the Mellor-Yamada Level II closure model. Practically speaking, this is the simplest of the models since, although it is more accurate than the Level 1 model, it is no more difficult to implement. For the Level II model, the tendency, advection and diffusion terms in the equations describing the conservation of the turbulent flux quantities are ignored. Hence, the turbulent flux quantities can be solved for algebraically.

For the Level II model, the turbulent kinetic energy equation is reduced to a balance between shear production, buoyancy production and dissipation, and is given by

$$0 = -\overline{u'w'}\frac{\partial U}{\partial z} - \overline{v'w'}\frac{\partial V}{\partial z} + \lambda\overline{\theta'w'} - \frac{q^3}{cl}, \quad (8)$$

where $q^2/2$ is the turbulent kinetic energy, l a turbulence length scale, and c a constant with a value of 15. The turbulent fluxes of momentum and heat can be written in eddy coefficient form as

$$-\overline{u'w'} = lq\mathrm{SM}\frac{\partial U}{\partial z}, \quad (9a)$$

$$-\overline{v'w'} = lq\mathrm{SM}\frac{\partial V}{\partial z}, \quad (9b)$$

$$-\overline{\theta'w'} = lq\mathrm{SH}\frac{\partial \theta}{\partial z}, \quad (10)$$

where SM and SH are particular functions of the local flux Richardson number Rf. The functions SM and SH are given by

$$\mathrm{SH} = 0.537 - 1.978\,\mathrm{Rf}/(1 - \mathrm{Rf}), \quad (11)$$

$$\mathrm{SM} = \mathrm{SH}\frac{[0.52 - 1.404\,\mathrm{Rf}/(1 - \mathrm{Rf})]}{[0.688 - 2.068\,\mathrm{Rf}/(1 - \mathrm{Rf})]}. \quad (12)$$

The flux Richardson number is given by $\mathrm{Rf} = (\mathrm{SH}/\mathrm{SM})\mathrm{Ri} = 0.725[\mathrm{Ri} + 0.186 - (\mathrm{Ri}^2 - 0.316\,\mathrm{Ri} + 0.0346)^{1/2}]$ (Mellor and Yamada, 1974), where Ri

is the Richardson number $\{=\lambda(\partial\theta/\partial z)[(\partial U/\partial z)^2 + (\partial V/\partial z)^2]^{-1}\}$.

The turbulence length scale l used by Mellor and Yamada (1974) is from Blackadar (1962) and is given by

$$l = kz(1 + kz/l_0)^{-1}, \tag{13}$$

when Karman's constant k is taken to be 0.4. The maximum scale length l_0 of the turbulence was parameterized by Mellor and Yamada as

$$l_0 = \gamma \int_0^\infty zqdz \Big/ \int_0^\infty qdz, \tag{14}$$

where γ is an empirical constant.

The values of the empirical constants used in the Level II model here are the same as those used in Mellor and Yamada (1974) with one exception. Mellor and Yamada set the constant γ in (12) equal to 0.10. We found that with $\gamma = 0.30$, the results for a neutrally stratified planetary boundary layer were in better agreement with values of u_* and α_0, the friction velocity and total Ekman veering, predicted using the standard similarity expression for these parameters [cf. Yamada, 1976, Eqs. (5a) and (6)] and the numerical constants in those expressions determined by Yamada (1976). Mellor and Durbin (1976) state that their results were fairly insensitive to γ (they varied γ from 0.05 to 0.10 but used $l = l_0$ throughout the boundary layer). We have noted the relative insensitivity of the Level II model to the value of γ in our own experiments (Martin, 1976).

b. *Method of solution*

Because of the large gradients that occur near the lower boundary, the equations were transformed to the logarithmic variable $\zeta = \ln z/z_0$ to provide adequate resolution near $z = z_0$. The resulting equations were solved on a vertical grid with a constant spacing in ζ between $\zeta = 0$ and $\zeta = \ln H/z_0$, where H was chosen large enough so that solutions were not affected by this "lid". The values of the diffusion coefficients were evaluated midway between the grid points at which the mean velocity and temperature were determined.

In this study we set z_0 equal to a constant rather than taking $z_0 = 0.1\,\nu/u_*$, i.e., we assume the bottom to be hydrodynamically rough rather than smooth. With a rough bottom assumed, ν and χ in (2)–(4) should be set equal to zero since no viscous conductive sublayer would then exist. However, our numerical scheme as coded becomes unstable with ν and χ set to zero, and in this study we have not set them equal to zero. Thus, our model predicts that for heights $\lesssim 0.1\nu/u_*$ above z_0 there is a viscous sublayer which of course is inconsistent with our assumption of a rough bottom. However, for the cases presented in this paper (we take $\nu = 10^{-6}\,\mathrm{m^2\,s^{-1}}$) $0.1\,\nu/u_* \approx z_0$. Thus the logarithmic speed profile, when extrapolated to zero speed, intersects the $\ln z$ axis at $\approx \ln 2z_0$ rather than at $\ln z_0$. Thus the net effect of our not setting $\nu = 0$ is to double z_0. As discussed later, the results presented here are fairly insensitive to the actual choice of roughness parameter.

With the bottom slope $\alpha = 0$, the momentum equations (2) are uncoupled from the heat equation (3). The resulting equations were solved using a forward time differencing scheme. The diffusion terms were evaluated at the new time level for stability and all other terms were averaged between the new and old time levels. The diffusion coefficients evaluated at the old time level were used at each iteration step. The heat equation in matrix form is then tridiagonal and was solved using the well known tridiagonal algorithm. The momentum equations in matrix form are block tridiagonal and were solved using a pentadiagonal matrix elimination scheme. With $\alpha \neq 0$, the value of temperature at the old time step in (2a) was used to determine U at the new time step, and in the heat equation (3) the value of U at the old time step was used.

"Steady" solutions were found by treating the problem as an initial value problem and integrating in time until the solutions became approximately steady. As discussed previously, the solutions are not completely steady and, depending on the value of α the temperature in the BBL slowly increases or decreases with time. To minimize oscillatory solutions associated with inertial motions, the driving term (the geostrophic velocity) was linearly started from zero at time zero to its final, constant value over a 2-day real-time interval.

The values of the friction velocity at u_* were determined by evaluating $(lq)^{1/2}[(\partial U/\partial z)^2 + (\partial V/\partial z)^2]^{1/4}$ at $z = z_0$. As a consistency check on the numerical algorithms, u_* was also estimated from integrating (2) from $z = z_0$ to $z = H$, i.e.,

$$\rho u_*^2 = [(\tau_0^x)^2 + (\tau_0^y)^2]^{1/2},$$

where

$$\tau_0^x = -\int_{z_0}^H (\partial U/\partial t - fV - \alpha\lambda\Theta)dz,$$

$$\tau_0^y = -\int_{z_0}^H (\partial V/\partial t + fU)dz.$$

The u_* values so computed were in agreement to at least seven significant figures.

5. Results

The problems we examine are illustrated in Fig. 5. We consider first the BBL for a steady current with no density stratification flowing over a flat, horizontal boundary (Fig. 5a). How this BBL is modified if the interior is stably stratified is then considered (Fig. 5b). Finally, including the effect of a

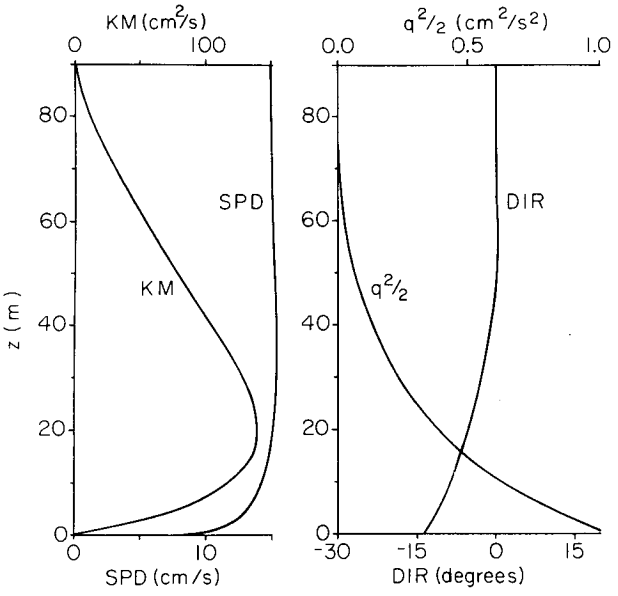

FIG. 6. Profiles of current speed (SPD), current direction (DIR), momentum diffusion coefficient (KM) and turbulent kinetic energy ($\frac{1}{2}q^2$) for the case depicted in Fig. 5a, $N_0^2 = 0$. Note the ambiguity in defining the depth of the BBL depending on which profile is used.

sloping bottom is examined (Figs. 5c and d). In all cases the interior geogstrophic current is taken as

$$U_g = 0, \tag{15a}$$

$$V_g = \begin{cases} (at)0.15 \text{ m s}^{-1}, & 0 \leq t \leq 2 \text{ days} \\ 0.15 \text{ m s}^{-1}, & t \leq 2 \text{ days} \end{cases} \tag{15b}$$

where $a = (2 \text{ days})^{-1}$. This ramp function for turning on the driving current was chosen to keep inertial oscillation motions negligible. A current of magnitude 0.15 m s^{-1} is representative for the data considered in Section 2. When $\alpha \neq 0$, Eq. (15) gives an interior flow aligned along isobaths. With $\alpha > 0$ (Fig. 5c) and $\mathbf{V}_g$ as given in (15), this corresponds to the northward interior flow described in Section 2. Conversely with $\alpha < 0$ (Fig. 5d), this corresponds to the southward flow described in Section 2. Recalling that the observations were made near a shelf break point (cf. Fig. 2), the upslope value of bottom slope 0.26×10^{-3} was chosen to be the appropriate α for "northward" flow (Fig. 5c) and minus the downslope value of 2.4×10^{-3} was taken to be the appropriate bottom slope for "southward" interior flow (Fig. 5d). The value of temperature stratification in the interior used in the runs depicted in Figs. 5b–5d is $S = 7 \times 10^{-2}$ °C m^{-1} and was chosen to give an interior Brunt-Vasäilä frequency $N_0 = 1.28 \times 10^{-2}$ s^{-1} appropriate for the interior conditions at the site discussed in Section 2. The Coriolis parameter used in these runs is $f = 0.63 \times 10^{-4}$ s^{-1}. The value of the roughness parameter z_0 used in all cases depicted in Fig. 5 was arbitrarily set to be 0.03 cm, a value determined by Weatherly (1972) for a site in the Florida Straits. Data collected at the site reported in Section 2, currently being analyzed by one of us (Weatherly), indicate that z_0 for this site is somewhat larger. However, the results presented here are not particularly sensitive to the choice of z_0. For example, increasing z_0 to 1 cm, a thirty-threefold increase, increases the BBL thickness by a factor of approximately only 2.

c. *The neutrally stratified case*

The results of the case depicted in Fig. 5a, i.e., $V_g = 0.15$ m s^{-1} and $S = \alpha = 0$, are depicted in Fig. 6. The value for the friction velocity u_* is 0.58 $\times 10^{-2}$ m s^{-1}. Fig. 6 illustrates the ambiguity in defining the depth of a planetary boundary layer formed in a neutrally stratified fluid. If one uses the speed profile the BBL thickness is about 30 m, which is near the conventional thickness given by (1) of $0.4\, u_*/f = 37$ m. Using the current direction profile gives a larger thickness of about 50 m. The KM [the diffusion coefficient for momentum (=lqSM)] and $q^2/2$ (the turbulent kinetic energy) profiles give a BBL thickness of ~85 m. Observationally, it is easier to measure speed profiles accurately than using either the direction KM or q^2 profiles, and it is clear why in the neutrally stratified case the thickness of the planetary boundary is taken to be $\sim 0.4\, u_*/f$. However, a physically more realistic thickness is that height at which the turbulence created in the boundary layer goes to zero. In terms of KH or q^2 this is the height at which KH = 0 and $q^2 = 0$. This corresponds to the height at which turbulent mixing goes to zero.

d. *The BBL over a non-sloping bottom with stratification case*

The results for the case illustrated in Fig. 5b with $V_g = 0.15$ m s^{-1}, $N_0 = 1.28 \times 10^{-2}$ s^{-1} and $\alpha = 0$ are shown in Fig. 7. The ambiguity in defining the BBL thickness when compared to the previous, neutrally stratified case is greatly reduced. Whether the speed, direction, KH, q^2 or temperature profiles are used, the BBL thickness is ~9 m. In addition to the BBL thickness being greatly reduced, KH and q^2 are also appreciably diminished. In Fig. 6, the maximum values of KH and $q^2/2$ are about 1.4×10^{-2} m^2 s^{-1} and 10^{-4} m^2 s^{-2}, while in Fig. 7 they are, respectively, about 0.2×10^{-2} m^2 s^{-1} and 10^{-5} m^2 s^{-2}.

In Fig. 7 the current direction profile is qualitatively similar to the temperature profile. Most of the direction changes occur at the top of the mixed layer where most of the temperature changes occur. In the mixed layer the current direction is more nearly constant. Comparison of the direction profiles in Figs. 6 and 7 shows that in the $N_0^2 > 0$ case the total Ekman

veering (27°) is about twice that for the $N_0^2 = 0$ case and furthermore that qualitatively the two direction profiles are quite different. The Ekman spiral form seen in Fig. 6 is not repeated in Fig. 7.

Thus, from Fig. 7 the BBL is seen to be a thermally well-mixed layer capped by what meteorologists would call an inversion. Furthermore, in the mixed layer the current flow is nearly unidirectional. Csanady (1974) analytically considered a similar problem, that of a well-mixed atmospheric boundary layer capped by an inversion. He assumed that the flow was nearly unidirectional in the mixed layer with most of the Ekman veering occurring in the inversion, and was able to show, subject to these assumptions, that

$$\sin\beta = u_*^2/fhV_g,$$

where β is the total Ekman veering and V_g the magnitude of the geostrophic flow. In contrast to the case considered here, the fluid above the inversion was taken to be neutrally stratified rather than stably stratified. Thus the density jump across the inversion could be specified independently of the mixed-layer depth h. In our case the density jump is determined by the value of h, a point we will return to later. By assuming a particular form for h (which is discussed in a later section) he was able to show that the Ekman veering β increased with increasing density contrast across the inversion (keeping everything else fixed) and that the limiting value for β was 90°. In light of this then, it is perhaps not unexpected that the total Ekman veering for the $N_0^2 > 0$ case (Fig. 7) was larger than for the $N_0^2 = 0$ case (Fig. 6).

The problem considered by Csanady (1974) is in many ways similar to that considered here and the results obtained in that study are helpful in interpreting why the total Ekman veering for the case depicted in Fig. 7 is greater than for the case shown in Fig. 6 where the fluid is everywhere neutrally stratified. However, the differences in the problem considered here and that by Csanady (1974) coupled with an assumption made by Csanady (1974) concerning the thickness of boundary layers require careful consideration before direct comparisons are made. We have attempted to analyze our problem in the same manner as done by Csanady (1974) and conclude, even if we accept his assumption about h, that we cannot arrive at his conclusions about the dependence of the Ekman veering on the density jump across the inversion and the limiting value of 90° without making an additional assumption about u_* and h. The difficulty arises because in our problem the density contrast across the inversion cannot be specified independently from h. Rather than presenting this analysis, we offer instead an alternative explanation for why the Ekman veering for the case $N_0^2 > 0$ (Fig. 6) is greater than for the case $N_0^2 = 0$ (Fig. 7). In so doing we must make the same assumption concerning u_* and h that are required if we proceed in the manner of Csanady (1974).

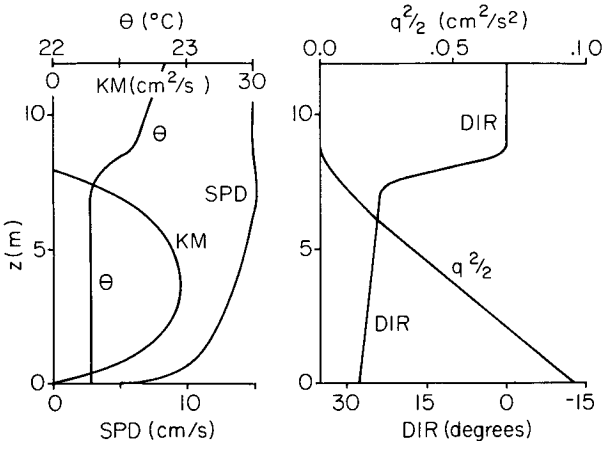

FIG. 7. Profiles of temperature (θ), current speed (SPD), current direction (DIR), momentum diffusion coefficient (KM) and turbulent energy ($\frac{1}{2}q^2$) for the case depicted in Fig. 5b. Note that the ambiguity in determining the depth of the BBL from the profiles seen in $N_0^2 = 0$ case (Fig. 6) is greatly reduced in this case.

The momentum equations for the BBL for the cases depicted in Figs. 6 and 7 are

$$-f(v - V_g) = \frac{1}{\rho}\frac{\partial \tau^x}{\partial z}, \qquad (2a')$$

$$fu = \frac{1}{\rho}\frac{\partial \tau^y}{\partial z}, \qquad (2b')$$

where u,v are the velocity components and τ^x, τ^y the stress components in the BBL [see Eq. (2)]. We introduce nondimensional stress components $T^x \equiv \tau^x/\rho u_*^2$, $T^y \equiv \tau^y/\rho u_*^2$ and a nondimensional vertical coordinate $\eta \equiv z/h$, and rewrite (2′) as

$$(fh/u_*^2)(V_g - v) = \partial T^x/\partial\eta, \qquad (2a'')$$

$$(fh/u_*^2)u = \partial T^y/\partial\eta. \qquad (2b'')$$

What we seek to determine is how u and v vary with varying N_0^2 from zero to some positive value (keeping f and V_g fixed) since $\beta = \tan^{-1}u/v$. It is reasonable to expect u_* and h to decrease as N_0 increases. If we assume that u_*^2 decreases at a slower rate than h as N_0^2 increases then we see from (2″) that for the left-hand side to balance the right hand that v must decrease and u must increase. Thus, the Ekman veering must increase as N_0^2 increases. The same result follows from (15) once this assumption is made; however, Eq. (15) is valid only for a mixed layer capped by an inversion. It follows from (2a″) and this assumption that as N_0^2 increases the Coriolis term in the x-momentum equation decreases relative to the pressure gradient term and the flow in the BBL is more down the pressure gradient. In the

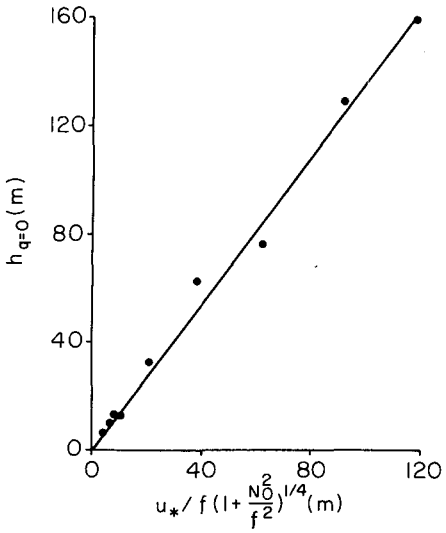

FIG. 8. Plot of the height above bottom at which $q = 0 (h_{q=0})$ as a function of $(u_*/f)[1 + (N_0^2/f^2]^{-1/4}$ for various values of V_g, f, N_0 and z_0. The values of $h_{q=0}$ and u_* were determined from the Mellor Level II model. The straight line is (17) with $A = 1.3$.

limiting case of N_0^2 very large it follows that the flow in the BBL is nearly down the pressure gradient, i.e., $\beta \approx 90°$. From (15) it then follows that as N_0^2 becomes very large u_*^2/h becomes nearly equal to $V_g f$.

Assuming that u_*^2 decreases proportionately at a slower rate with increasing N_0^2 than does h is equivalent to assuming that the major effect to the BBL of introducing a nonzero N_0^2 is to decrease the thickness of the layer rather than to decrease the level of turbulence in the layer (since $q^2 \approx u_*^2$). After the BBL has formed, the work done against the buoyancy force is small in the mixed layer and only appreciable in the inversion. Thus, as long as the thickness of the inversion remains small in comparison to the thickness of the mixed layer such an assumption seems reasonable. The assumption is borne out by the Level II model. For the run depicted in Fig. 7 $u_* = 0.55 \times 10^{-2}$ m s^{-1}, a reduction of about 5% from the $N_0^2 = 0$ case. Thus u_*^2 has been reduced by about 10%, while h has been reduced by at least 60%. The BBL thickness for the $N_0^2 > 0$ case is then considerably less than $0.4\, u_*/f$. It is therefore pertinent to digress and consider the general question of what is the thickness of a BBL formed in a stably stratified ocean before considering how the BBL depicted in Fig. 7 is modified by allowing the bottom to be inclined.

e. What is the thickness of the BBL formed in a stably stratified ocean?

As noted earlier the thickness of the turbulent Ekman layer formed above the ocean's bottom is often taken to be $h \approx 0.4\, u_*/f$. The results presented in the preceding paragraphs suggest that this relation may not in general apply for BBL formed in a stably stratified ocean. We offer the following, which is based solely on dimensional grounds, as an expression for the thickness of such a BBL:

$$h = Au_*/f(1 + N_0^2/f^2)^{1/4}, \qquad (17)$$

where A is a constant and N_0 the Brunt-Vasäilä frequency of the water in the interior outside the BBL. The above relation reduces to $h \approx Au_*/f$ for $N_0 \ll f$ and $h \approx Au_*/(fN_0)^{1/2}$ for $N_0 \gg f$. The former expression is of the correct form for planetary boundary layers formed in neutrally stratified fluids and the latter resembles the thickness of the surface wind-mixed layer derived from slab models (cf. Pollard *et al.*, 1973).

We take the thickness of the BBL to be that height at which the turbulent kinetic energy, or equivalently, the turbulent mixing, goes to zero, and denote this height as $h_{q=0}$. In Fig. 8 we present values of $h_{q=0}$, as determined from the Level II model for various values of the input parameters V_g, f, z_0 and N_0, plotted as a function of $u_*/f[1 + (N_0^2/f^2)]^{1/4}$, where u_* is also determined from the Level II model. We see that for the range of parameters considered (17) closely approximates $h_{q=0}$ provided $A \approx 1.3$. Thus we rewrite (17) as

$$h = 1.3\, u_*/f[1 + (N_0^2/f^2)]^{1/4}. \qquad (17')$$

Plotted in Fig. 8 is a point corresponding to the results presented in Fig. 7. Thus the observations and numerical model gives values of BBL thickness which are comparable (~10 m), appreciably smaller than $0.4\, u_*/f$, but in agreement with (17').

We note that (17) can be written, based on dimensional grounds, as $h = (Au_*/f)\Phi(N_0/f)$, where Φ is some function of N_0/f which must approach 1 as N_0 approaches zero. In (17) Φ is approximated by the expression $[1 + (N_0^2/f^2)]^{1/4}$. For the runs given in Fig. 8 the ratio N_0^2/f^2 ranges from 0 to about 200. Thus for these values of N_0^2/f^2, $\Phi \approx [1 + (N_0^2/f^2)]^{1/4}$; however, for $N_0^2/f^2 \gg 200$ this may not be a valid approximation to Φ. Finally, we point out that the form chosen for h by Csanady (1974) is equivalent to choosing $\Phi = N_0/f$ which gives $h = Au_*/N_0$ which is independent of f.

f. The BBL over a sloping bottom

The cases depicted in Figs. 5c and 5d are considered. The only difference from the case shown in Fig. 5b is that the bottom slope is nonzero; for Fig. 5c $\alpha = 0.26 \times 10^{-3}$ and for Fig. 5d $\alpha = -2.4 \times 10^{-3}$. In each case, 5-day runs were made. During the first 2 days, the geostrophic current was turned on linearly; once it reached 0.15 m s^{-1} at time = 48 h, it was kept fixed at that value (cf. Fig. 9b). As dis-

cussed in Section 3, the temperature in the BBL is expected to increase or decrease with time depending on the sign of α. This behavior can be seen in Fig. 9c, where temperature profiles are drawn at the beginning of each 24 h period. The dashed curves are for the case $\alpha = 0.26 \times 10^{-3}$ (Fig. 5c) and the solid curves are for the case $\alpha = -2.4 \times 10^{-3}$ (Fig. 5d). The temperature of the mixed layer is shown as a function of time in Fig. 9a. As might be expected from (3) and confirmed in Fig. 9, $|\partial\theta/\partial t|$ in the BBL is directly proportional to $|\alpha|$. In the case of downwelling of warmer water (the dashed profiles in Fig. 9c) the BBL thickness is seen to slowly increase with time, while in the case of upwelling of cooler water the BBL thickness remains constant. Thus, in a case where upwelling may be occurring, the BBL thickness is approximately given by (17′), while in a case where downwelling may be occurring the BBL thickness may be appreciably larger than that given by (17′). In either case the BBL does not have the simple signature of a layer formed by simple mixing (cf. Fig. 6).

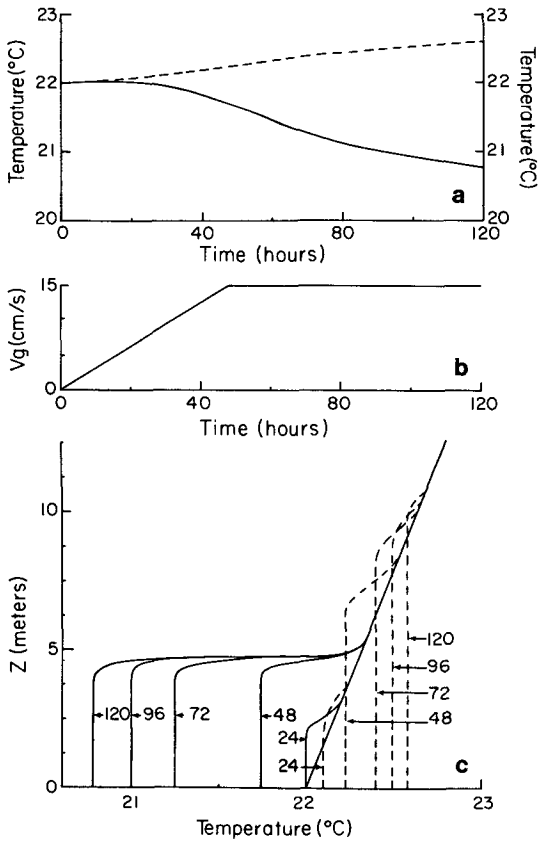

FIG. 9. Time series (a) of the temperature of the bottom mixed layer as a function of time for V_g as indicated in (b), and temperature profiles (c) at times 0, 24, 48, 72, 96 h. Solid curves are for the case $\alpha = 0.26 \times 10^{-3}$ (Fig. 5c) and the dashed curves are for the case $\alpha = -2.6 \times 10^{-3}$ (Fig. 5d). Note that the BBL thickness increases with time in the case of downwelling.

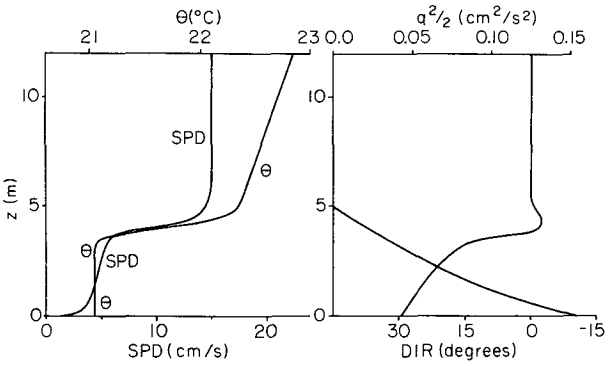

FIG. 10. Profiles of temperature (θ), current speed (SPD), current direction (DIR), momentum diffusion coefficient (KM) and turbulent kinetic energy ($\frac{1}{2}q^2$) for the case $\alpha = -2.6 \times 10^{-3}$ (Fig. 5d).

We do not present a figure for the downwelling case, since it is very similar to Fig. 7. The total Ekman veering is somewhat reduced (by ~5°). Fig. 10 shows profiles of speed, temperature, current direction, momentum diffusion coefficient and turbulent kinetic energy for Day 4 in the case of upwelling (Fig. 5d). Some of the features seen in Fig. 1d are seen. The temperature and direction profiles are qualitatively very similar. There is a jet-like feature in the direction profile. A lens of cold water is seen immediately above the bottom. As reported in I, the total Ekman veering was largest in the case of southerly flow. Comparing Figs. 7 and 9 and the comparable figure for the case illustrated in Fig. 5c (but not shown here), the predicted veering is also largest for the case of upwelling in the "southerly" flow.

Qualitatively, the Mellor Level II model predicts results in very good agreement with the observations reported in I. The thickness of the BBL is appreciably less (~5–10 m) than that expected for a BBL formed in a neutrally stratified fluid (~30 m). Including a sloping bottom gives results similar to those shown in Fig. 2 in that the temperature in the BBL is seen to slowly increase with time when the interior current flows northward and to decrease with time at a faster absolute rate when the interior flow is southward. In agreement with I, the total Ekman veering in the case of southward flow is greater than in the case of northward flow. The predicted temperature, speed and current direction profiles are similar to those observed.

Once a mixed layer has formed in the sloping bottom case the density field in the BBL is no longer horizontally homogeneous. Thus a "thermal wind shear" is induced in the BBL. We have neglected this effect, i.e., we have taken V_g to be constant throughout the BBL. The computed ΔV_g across the BBL for the case depicted in Fig. 5c (the downwelling case) due to this thermal wind shear is

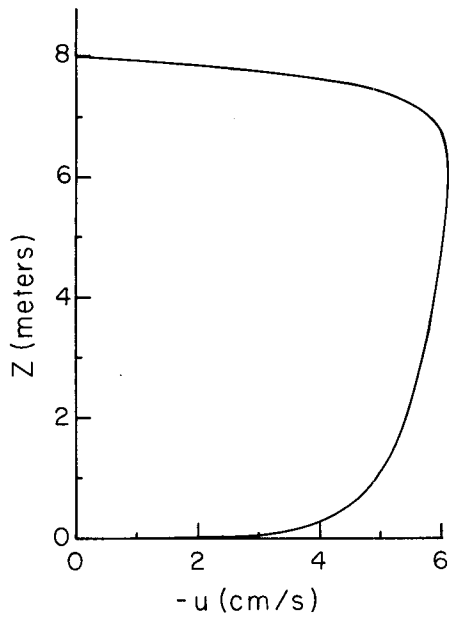

FIG. 11. Profile of the cross-isobaric velocity component u in the BBL for the case $\alpha = 0$, $N_0 \neq 0$ (Fig. 5b) summarized in Fig. 7.

small ($<10^{-2}$ m s^{-1}). Thus, for this case, and because of the limited time scale considered, this is probably not a serious omission. However, while the computed ΔV_g across the mixed layer due to the thermal wind effect for the upwelling case (Fig. 5d) is also comparably small, the ΔV_g across the interior becomes large ($\sim$0.10 m s^{-1}) by the end of the 5-day run. Thus the results for the upwelling case are suspect in the latter half of the experiment. Since this shear is such to reduce V_g in the mixed layer, the rate of cooling of the mixed layer for the upwelling case as shown in Fig. 9 is probably overestimated in the latter part of the experiment.

g. Stability of the BBL

Armi and Millard (1976) propose that the turbulent Ekman layer in the vicinity of the MODE area in the western North Atlantic Ocean is unstable in a Froude number sense. Their arguments are somewhat tenuous due to assumptions made about the slab-like structure of the layer and due to the assumption that Froude number criteria developed for nonrotating reference frames apply to the BBL where the Coriolis effect is clearly important.

From Figs. 1 and 7 it is apparent from the speed profiles that the BBL does not move as a slab even though temperature or direction profiles suggest slab-like behavior. From the jet-like structure in the speed profile, it could be argued that there is a discontinuity in the speed at the top of the BBL and the interior speed. However, this "jump" in speed is about 0.01 m s^{-1} and is much less than the speed c of interficial gravity waves associated with the density jump at the top of the mixed layer [$c = (g'h)^{1/2} = 0.06$ m s^{-1}, where $g' = g\Delta\rho/\rho$ is the reduced gravity, $\Delta\rho$ the density difference across the top of the BBL, ρ the density of the mixed layer, and h the thickness of the bottom mixed layer]. Thus a Froude number formed by taking the ratio of the "jump" in the speed at the top of the BBL (0.01 m s^{-1}) to $c = (g'h)^{1/2} = 0.06$ m s^{-1} is appreciably less than 1.

If Froude-number-associated instabilities are to be sought in a planetary boundary layer, it is more appropriate to consider the down-the-pressure-gradient component of the velocity profile rather than the speed profile of the boundary layer or the along-isobars velocity profile, which resembles the latter profile. In the case of interest here, this is the u or cross-isobaric velocity profile, and for the stratified, nonsloping bottom case summarized in Fig. 7, the $u(z)$ profile is presented in Fig. 11. In terms of the cross-isobaric component, the BBL is seen to resemble a slab. Fig. 11 closely resembles Fig. 4.17 in Turner (1973). The latter figure is a sketch of the gravity-driven flow of a heavy layer down a slope, and in subsequent review of the stability of such flows, the heavy layer is considered as a slab of thickness h moving at the speed $\bar{u}$, the vertically averaged downslope speed, capped by a density "jump" $\Delta\rho$. Citing experimental evidence, Turner (1973) concludes such layers are unstable when the Froude number

$$F \equiv \bar{u}/(g'h)^{1/2} > 1.$$

The corresponding value of F for the case depicted in Figs. 7 and 11 where $(g'h)^{1/2} = 0.06$ m s^{-1} and $\bar{u} = 0.05$ m s^{-1} is 0.83. Thus for the case studied $F < 1$, which implies (following Turner, 1973) that the BBL is stable in a Froude number sense. That the observed BBL thickness is comparable to that predicted by the Mellor Level II model suggests that the actual BBL was indeed stable in a Froude number sense.

While $F < 1$ for the case considered, the fact that it was nearly equal to 1 suggests that with different values of the external parameters $\mathbf{V}_g$, f, N_0, z_0 the oceanic BBL may be supercritical, i.e., $F > 1$. Thus while the model and the data indicate that the BBL on the western Florida Shelf at the time and site considered here was stable, the BBL elsewhere may be supercritical. We have used as input parameters for the model values thought to be representative for two other sites: the BBL of the Florida Current (Weatherly, 1972) and the BBL in the western North Atlantic (Armí and Millard, 1976). For the former, the external parameters chosen were $V_g = 0.20$ m s^{-1}, $N_0 = 1.88 \times 10^{-3}$ s^{-1}, $f = 0.63 \times 10^{-4}$ s^{-1} and $z_0 = 3 \times 10^{-4}$ m; and for the latter $V_g = 0.15$ m s^{-1}, $N_0 = 7 \times 10^{-4}$ s^{-1}, $f = 0.68 \times 10^{-2}$ and

$z_0 = 3 \times 10^{-5}$ m. For the Florida Current the resulting Froude number F = 1.0 and for the western North Atlantic F = 1.4. Thus the BBL for the Florida Current appears to be marginally stable, while that for the western North Atlantic appears to be supercritical. We have run tests with other values of the input parameters and tentatively conclude that for conditions of stronger currents and larger N_0 characteristics of continental margins in nonwinter months the BBL is marginally stable or stable ($F \lesssim 1$), while for conditions of weaker currents and smaller N_0 characteristic of the deep ocean the BBL is supercritical ($F > 1$).

6. Summary and conclusions

We have tested the Level II model of Mellor and Yamada (1974) against data from the BBL on the western Florida Continental Shelf with encouraging results. The predicted BBL thickness compares favorably with that observed (6–12 m) and is appreciably less than the thickness expected for a BBL formed in neutrally stratified fluid (~30 m). That the thickness is less is attributed to the BBL being formed in a stably stratified water column. The Level II model suggests that the density stratification of the water in which the BBL is formed, i.e., the density stratification just above the BBL in the interior, markedly reduces the thickness of the BBL. In Section 5 we suggested that the BBL thickness be identified with that height above the bottom at which the turbulent kinetic energy generated in the BBL goes to zero. This should be the height at which turbulent mixing goes to zero. On dimensional grounds we proposed that this thickness is approximated by $h_{q=0} = (Au_*/f)[1 + (N_0^2/f^2]^{-1/4}$, where N_0 is the Brunt-Vasäilä frequency in the interior, and have used the Level II model to determine that $A = 1.3$. The Level II model indicates that the above expression is a good approximation for $0 \leq N_0^2/f^2 \leq 200$.

We have also tested an idea proposed in Weatherly and Van Leer (1977) that the observed local heating (cooling) in the BBL relative to the interior could be due to Ekman-veering-induced downwelling (upwelling) of water in the BBL. The model gives results in good qualitative agreement with their observations in that $|\partial\theta/\partial t|$ for southerly flow is much larger than for northerly flow. The model suggests that the temperature of the bottom mixed layer cannot be accounted for by simple vertical mixing for the BBL formed in a stratified flow for the case where the isotherms are not parallel to the bottom. Advective motions upslope or downslope in the BBL can result in appreciable local cooling or heating of the BBL.

The use of the Level II model permits the vertical distributions of the current speed and direction, temperature and turbulent exchange coefficients and turbulent kinetic energy in the BBL to be investigated. Features common to both the observations and the predicted results are that most of the current direction changes occur at the top of the BBL where the density stratification is largest, that the direction and temperature profiles are very similar, that the total Ekman veerings are greater than that expected for a BBL formed in a neutrally stratified fluid, that at times there is a "jet" structure to the speed and direction profiles, and that while the direction and temperature profiles suggest a slab-like behavior to the BBL, the speed profiles suggest that the BBL does not move as a slab.

Although the speed profiles (and along-isobaric v profiles) do not indicate that the BBL moves as a slab, the cross-isobaric or down-the-pressure-gradient u profile does resemble a slab very similar to the gravity-driven flow of a heavy fluid down a slope discussed by Turner (1973). Such flows are unstable when $F \equiv \bar{u}(g'h)^{1/2} > 1$ (Turner, 1973); here $\bar{u}$ is the vertically averaged down-the-pressure-gradient flow, g' the reduced gravity and h the layer thickness. The BBL's displayed in Figs. 1, 7 and 10 are stable in the sense that $F < 1$. Other runs made with the model give an F for the BBL formed on continental margins where the water column is stably stratified and currents ~10 m s^{-1} that is subcritical or marginally critical ($F \lesssim 1$), and an $F > 1$ for the BBL for the deep ocean where the currents and the density stratification of the overlying water are weaker.

Acknowledgments. We are very grateful for helpful discussions with Drs. Steve Blumsack [who suggested Eq. (17)], Ya Hsueh, James O'Brien and Wilton Sturges III. We thank an anonymous reviewer for his substantive and constructive criticisms, and Dr. Robert Grace for his assistance in programming. This research was sponsored by the Office of Naval Research under Contract N000-14-75-C-0201.

REFERENCES

Armi, L., and R. C. Millard, Jr., 1976: The bottom boundary layer of the deep ocean. *J. Geophys. Res.*, **81**, 4983–4990.

Blackadar, A. K., 1962: The vertical distribution of wind and turbulent exchange in a neutral atmosphere. *J. Geophys. Res.*, **67**, 3095–3102.

Businger, J. A., and S. P. S. Arya, 1974: Height of the mixed layer in the stably stratified atmospheric boundary layer. *Advances in Geophysics*, Vol. 18A, F. N. Frenkiel and R. E. Munn, Eds., Academic Press, 73–92.

Caldwell, D. R., 1976: Fine-scale temperature structure in the bottom mixed layer on the Oregon shelf. *Deep-Sea Res.*, **23**, 1025–1036.

Csanady, G. T. 1974: Equilibrium theory of the planetary boundary layer with an inversion lid. *Bound-Layer Meteor.*, **6**, 63–69.

Frenkiel, F. N., and R. E. Munn, 1974: *Advances in Geo-*

physics, Vol. 18A, F. N. Frenkiel, and R. E. Munn, Eds., Academic Press, 462. pp.

Hsueh, Y., 1969: Buoyant Ekman layer. *Phys. Fluids*, **12**, 1757–1762.

Kolmogoroff, A. N. 1941: The local structure of turbulence in incompressible viscous fluids for large Reynolds number. *C. R. Akad. Nauk SSSR*, **30**, 301–305. Translation, Friedlander, S. K. and L. Topper, Eds., 1961: *Turbulence, Classic Papers on Statistical Theory*, Interscience.

Kundu, P. K. 1976: Ekman veering observed near the ocean bottom, *J. Phys. Oceanogr.*, **6**, 238–242.

Lykosov, V. H., and L. N. Gutman, 1972: Turbulent boundary layer over a sloping underlying surface. *Izv. Adak. Nauk USSR Fiz. Atmos Okeana*, **8**, 799–809.

Martin, P. J., 1976: A comparison of three diffusion models of the upper mixed layer of the ocean. Naval Research Laboratory, Memo. Rep. 3399', Washington, D. C., 53 pp.

Mellor, G. L., and T. Yamada, 1974: A hierarchy of turbulence closure models for planetary boundary layers. *J. Atmos. Sci.*, **31**, 1791–1806.

——, and P. A. Durbin, 1975: The structure and dynamics of the ocean surface mixed layer. *J. Phys. Oceanogr.*, **5**, 718–728.

Mercado, A., and J. Van Leer, 1976: Near bottom velocity and temperature profiles observed by cyclosonde. *Geophys. Res. Lett.*, **3**, 633–636.

Pollard, R. T., R. B. Rhines, and R. O. R. Y. Thompson, 1973: The deepening of the wind-mixed layer. *Geophys. Fluid Dyn.*, **3**, 381–404.

Rotta, J. C., 1951: Statische theorie nichthomogener turbulenz. *Z. Phys.*, **129**, 547–572; **131**, 51–77.

Turner, J. S., 1973: *Buoyancy Effects in Fluids*. Cambridge University Press, 357 pp.

Vager, B. G., and S. S. Zilitinkevich, 1968: A theoretical model of diurnally varying meteorological fields. *Meteor. Gidrol.*, No. 7.

Van Leer, J., W. Duing, R. Erath, E. Kennelly and A. Speidel, 1974: The cyclosonde: an unattended vertical profiler for scalar and vector quantities in the upper ocean. *Deep-Sea Res.*, **21**, 385–400.

Weatherly, G. L., 1972: A study of the bottom boundary layer of the Florica Current. *J. Phys. Oceanogr.*, **2**, 54–72.

——, 1975: A numerical study of time-dependent turbulent Ekman layers over horizontal and sloping bottoms. *J. Phys. Oceanogr.*, **5**, 288–299.

——, and J. Van Leer, 1977: On the importance of stable stratification to the structure of the bottom boundary layer on the western Florida Shelf. *Bottom Turbulence*, J. Nihoul, Ed., Elsevier, 103–122.

Wimbush, M., and W. Munk, 1970: The benthic boundary layer. *The Sea*, Vol. 4, Part 1, Wiley, 731–758.

Yamada, T. 1976: On the similarity functions *A*, *B* and *C* of the planetary boundary layer. *J. Atmos. Sci.*, **33**, 701–780.

Zilitinkevich, S. S., 1972: On the determination of the height of the Ekman boundary layer. *Bound.-Layer Meteor.*, **3**, 141–145.